Control of the patterns by using time-delayed feedback near the codimension-three Turing–Hopf–Wave bifurcations*

Wang Hui-Juan(王慧娟)†, Wang Yong-Jie(王永杰), and Ren Zhi(任 芝)

School of Mathematics and Physics, North China Electric Power University, Baoding 071003, *China*

(Received 27 July 2013; revised manuscript received 22 September 2013)

Control of the spatiotemporal patterns near the codimension-three Turing–Hopf–Wave bifurcations is studied by using time-delayed feedback in a three-variable Brusselator model. Linear stability analysis of the system shows that the competition among the Turing-, Hopf- and Wave-modes, the wavenumber, and the oscillation frequency of patterns can be controlled by changing the feedback parameters. The role of the feedback intensity P_u played on controlling the pattern competition is equivalent to that of P_w, but opposite to that of P_v. The role of the feedback intensity P_u played on controlling the wavenumber and oscillation frequency of patterns is equivalent to that of P_v, but opposite to that of P_w. When the intensities of feedback are applied equally, changing the delayed time could not alter the competition among these modes, however, it can control the oscillation frequency of patterns. The analytical results are verified by two-dimensional (2D) numerical simulations.

Keywords: pattern formation, reaction diffusion system, time-delayed feedback

PACS: 05.45.−a, 82.40.Ck, 47.54.−r **DOI:** 10.1088/1674-1056/22/12/120503

1. Introduction

Spatiotemporal patterns which form through self-organization exist in a variety of physical, chemical, and biological systems.[1–7] The study of the dynamics of pattern formation has attracted much attention in different fields because these patterns exhibit certain similarities although their origins are very different. From the linear stability analyses, these patterns result from three types of bifurcations: Turing-, Hopf-, and Wave-bifurcations. Turing bifurcation breaks the spatial symmetry, which leads to stationary periodical patterns. Hopf bifurcation breaks the temporal symmetry, which leads to uniformly oscillatory patterns. Wave bifurcation breaks both the spatial and the temporal symmetries, which results in spatiotemporal patterns. These bifurcations could appear to have simultaneously resulted in considerably complex patterns.[1,4,5]

One aim of studying the dynamics of pattern formation is to realize the control of the patterns. Biological experiments have shown that spiral waves of electrical activity are related to life-threatening cardiac arrhythmias. Therefore, how to control and eliminate the spiral waves of electrical activity is currently a hot topic in cardiology research. Many strategies have been proposed to control the spatiotemporal patterns with different characteristics of dynamics.[8–20] Guo *et al.* studied the control of spiral waves by using local feedback in a light-sensitive Belousov–Zhabotinsky reaction.[8] Spiral turbulence was prevented by introducing local inhomogeneities around a small area of spiral tips. Zhang *et al.* realized the suppression of spiral turbulence by applying a periodical signal acted locally on the media.[11] Recently, Sen *et al.* studied the global control of spiral waves by using time-delayed feedback.[17]

At present, the studies on the control of the patterns mainly focus on that in excitable and bistable systems. In the oscillatory system, that is confined to the region near the codimension-two Turing–Hopf bifurcations.[21–25] Li *et al.* observed an oscillatory superlattice pattern which resulted from the interaction between the Turing and Hopf modes.[22] He *et al.* studied the transition between the Turing and antispiral patterns by using time-delayed feedback.[18] Because Wave bifurcation could induce complex patterns, the study on the spatiotemporal patterns near the codimension-three Turing–Hopf–Wave bifurcations has attracted much attention in the past decade.[1,4,5] One open question is how to control effectively the pattern formation near the codimension-three Turing–Hopf–Wave bifurcations. In this work, we study the control of the spatiotemporal patterns near the codimension-three Turing–Hopf–Wave bifurcations by using the strategy of time-delayed feedback. The effect of the time-delayed feedback on the wavenumber and the oscillatory frequency of patterns are discussed based on the linear stability analyses. The roles of time-delayed feedback played on controlling the Turing-, Hopf-, and Wave-modes are confirmed. The analytical results are verified well by numerical simulations.

2. Reaction–diffusion model

In order to study the effect of time-delayed feedback on controlling the pattern formation near the codimension-three Turing–Hopf–Wave bifurcations, we adopt a modified three-

*Project supported by the National Nature Science Foundation of China (Grant No. 11205044) and the Fundamental Research Funds for the Central Universities (Grant No. 10ML40).

†Corresponding author. E-mail: whuijuanmail@126.com

© 2013 Chinese Physical Society and IOP Publishing Ltd

variable Brusselator model expressed as follows:

$$\frac{\partial u}{\partial t} = f(u,v,w) + D_u\nabla^2 u + F, \quad (1)$$

$$\frac{\partial v}{\partial t} = g(u,v,w) + D_v\nabla^2 v + G, \quad (2)$$

$$\frac{\partial w}{\partial t} = h(u,v,w) + D_w\nabla^2 w + H, \quad (3)$$

where, the reaction terms $f(u,v,w)$, $g(u,v,w)$, and $h(u,v,w)$ are expressed as:

$$f(u,v,w) = a-(1+b)u+u^2v-cu+dw, \quad (4)$$

$$g(u,v,w) = bu-u^2v, \quad (5)$$

$$h(u,v,w) = cu-dw. \quad (6)$$

Here u, v, and w are dimensionless variables, which correspond to the concentrations of the activator, inhibitor, and unreactive species, respectively. D_u, D_v, and D_w denote their diffusion coefficients, respectively. Parameters a, b, c, and d are rescaled kinetic parameters. The variable w represents an unreactive form of u, and it does not take part in any chemical reactions.[26] The introduction of the new variable w could lead to Wave bifurcation. To study the competition of the spatiotemporal patterns near the codimension-three Turing–Hopf–Wave bifurcations, the diffusion coefficients D_u, D_v, D_w are taken as $D_u < D_v < D_w$ in this work. The terms F, G, and H in Eqs. (1)–(3) refer to the applied time-delayed feedback with the forms

$$F = P_u[u(t-\tau)-u(t)], \quad (7)$$

$$G = P_v[v(t-\tau)-v(t)], \quad (8)$$

$$H = P_w[w(t-\tau)-w(t)], \quad (9)$$

where P_u, P_v, and P_w represent the feedback intensities of u, v, and w, respectively. τ is the delayed time of the feedback. In this work, we consider τ as a small quantity. So the feedback terms of Eqs. (7)–(9) can be expanded in matrix form as:

$$\Psi(t-\tau)-\Psi(t) = -\tau\frac{\partial\Psi}{\partial t}, \quad (10)$$

here, $\Psi = [u,v,w]^{\mathrm{T}}$. Inserting Eq. (10) into the model equations (1)–(3), we can obtain the following matrix

$$P\partial_t\Psi = Q + D\nabla^2\Psi. \quad (11)$$

The principal elements P_{ii} of the diagonal matrix P are $[(1+\tau P_u),(1+\tau P_v),(1+\tau P_w)]$, which are related with feedback parameters. $Q = [f,g,h]^{\mathrm{T}}$ represents the nonlinear reaction term, i.e., Eqs. (4)–(6). The principal elements D_{ii} of the diagonal matrix D are the diffusion coefficients $[D_u,D_v,D_w]$. The homogeneous steady states of Eqs. (1)–(3) are

$$\Psi_0 = \left[a, \frac{b}{a}, \frac{ac}{d}\right]^{\mathrm{T}}.$$

Applying small spatiotemporal perturbations $\Delta\Psi = [\Delta u,\Delta v,\Delta w]^{\mathrm{T}}$ to the homogeneous steady states, $\Psi = \Psi_0 + \Delta\Psi$, and linearizing the dynamical system, we obtain:

$$P\partial_t\Delta\Psi = A\Delta\Psi + D\nabla^2\Delta\Psi. \quad (12)$$

Here, the principal elements A_{ii} of the diagonal matrix A can be written in the form

$$A_{ii} = \frac{\partial Q_i}{\partial\Psi_j}\Big|_{\Psi_0}, \quad (i,j)\in(1,2,3).$$

By expressing spatiotemporal perturbation in Fourier's space,

$$\Delta\Psi = \sum_k C\mathrm{e}^{\lambda t+\mathrm{i}kx},$$

here $C = [c_k^1,c_k^2,c_k^3]^{\mathrm{T}}$, we obtain the following matrix equation for eigenvalues of the stability matrix

$$\lambda C = (A-B)C. \quad (13)$$

The principal elements of the diagonal matrix B read $B_{ii} = k^2D_{ii} + P_{ii}\lambda$. By expanding Eq. (13) we obtain a cubic equation about the eigenvalues λ, and can further discuss the stabilities of the homogeneous steady states by using linear stability analysis.

Based on the linear stability analysis of the homogeneous steady states, we obtain the bifurcation diagram without time-delayed feedback as shown in Fig. 1. Turing bifurcation occurs at $\mathrm{Im}(\lambda_{k\neq0}) = 0$, $\mathrm{Re}(\lambda_{k\neq0}) = 0$, as indicated by the solid line. Wave bifurcation occurs at $\mathrm{Im}(\lambda_{k\neq0}) \neq 0$, $\mathrm{Re}(\lambda_{k\neq0}) = 0$, as indicated by the dashed line. Hopf bifurcation occurs at $\mathrm{Im}(\lambda_{k=0}) \neq 0$, $\mathrm{Re}(\lambda_{k=0}) = 0$, as indicated by the dash–dotted line. It is obvious that the parameter space is divided into six domains by the three bifurcation lines. In domain I, the homogeneous steady state is the only solution. Domains II and III are pure Turing and pure Wave regions, respectively. Turing and Wave instabilities coexist in the domain IV. Hopf and Wave instabilities arise in domain V. In domain VI the three instabilities occur simultaneously. In the following, we will focus on the dynamic of patterns in domain VI, where the three instabilities coexist, and investigate the role of time-delayed feedback played on controlling the spatiotemporal pattern.

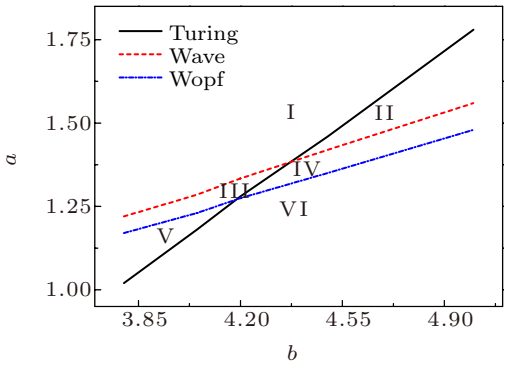


Fig. 1. (color online) Bifurcation diagram for b–a parameter space without the time-delayed feedback. Other parameters are $D_u = 1.7$, $D_v = 12.1$, $D_w = 160$, $c = d = 1.5$.

First, we analyze the effect of the feedback intensity P_u on the three modes (with fixed $P_v = P_w = 0$). Figure 2 shows the dispersion relation with different P_u. It can be seen that the three modes are affected by P_u. The characteristics of the Hopf and Wave modes change more remarkably than that of the Turing mode. The intensities of the Hopf and Wave modes

decrease rapidly with increasing P_u as shown in Fig. 3(a). Because the formation of a pattern with certain symmetry is mainly determined by the intensities of these modes, by applying appropriate P_u one can change the intensities of these modes and thereby control the pattern formation resulted from the competition between the three modes. In addition, the feedback intensity can also change the oscillation frequency and intrinsic wavenumber of patterns, as shown in Figs. 3(b) and 3(c). For Wave mode, both the oscillation frequency (solid line in Fig. 3(b)) and the intrinsic wavenumber (solid line in Fig. 3(c)) decrease with P_u. The oscillation frequency of the Hopf mode (dashed line in Fig. 3(b)) also decreases with P_u. However, there is little effect of feedback intensity P_u on the intrinsic wavenumber of the Turing mode (dashed line in Fig. 3(c)).

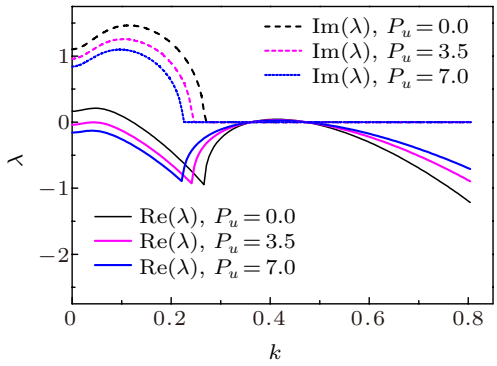


Fig. 2. (color online) Dispersion relation with different feedback intensities $P_u = 0.0, 3.5, 7$. The solid and dashed lines correspond to the real and image parts of the eigenvalues λ, respectively. Other parameters are $D_u = 1.7$, $D_v = 12.1$, $D_w = 160$, $a = 1.15$, $b = 4.05$, $c = d = 1.5$, $\tau = 0.1$, $P_v = P_w = 0$.

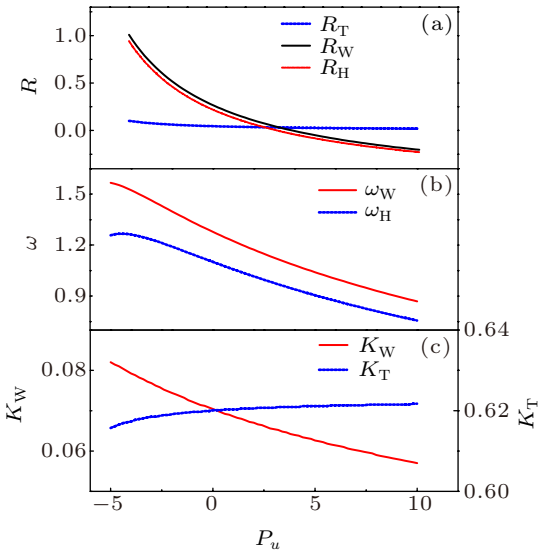


Fig. 3. (color online) Dependence of the intensities of the Turing, Hopf, and Wave modes (a), the oscillation frequency of the Wave and Hopf modes (b), the intrinsic wavenumber of the Turing and Wave modes (c) on P_u. Other parameters are $D_u = 1.7$, $D_v = 12.1$, $D_w = 160$, $a = 1.15$, $b = 4.05$, $c = d = 1.5$, $\tau = 0.1$, $P_v = P_w = 0$.

In order to compare the effect of the feedback intensity P_v on controlling the pattern formation with that of P_u, we then study the role of P_v played on controlling the three modes. Figure 4(a) shows the dependence of intensities of the three modes on P_v with fixed $P_u = P_w = 0$. It can be seen that the intensities of the Wave and Hopf modes increase rapidly with P_v, while the intensity of the Turing mode increases slightly with P_v. It shows that the effect of P_v on the intensities of the modes is opposite to that of P_u. This is because that variables u and v are the activator and inhibitor of the system, respectively, and the actions of them on the system are opposite. Therefore the feedback of u and v also play opposite roles on controlling the intensities of the three modes. The dependencies of the oscillation frequency and the intrinsic wavenumber of the patterns on P_v are shown in Figs. 4(b) and 4(c), respectively. It can be seen that both the oscillation frequency (solid line in Fig. 4(b)) and the intrinsic wavenumber (solid line in Fig. 4(c)) of the wave mode decrease with P_v. The oscillation frequency of the Hopf mode (dashed line in Fig. 4(b)) also decreases with P_v. The intrinsic wavenumber of the Turing mode decreases slightly with P_v.

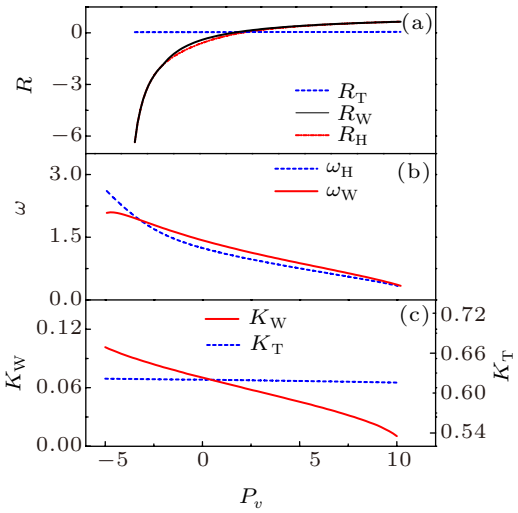


Fig. 4. (color online) Dependence of the intensities of the Turing, Hopf, and Wave modes (a), the oscillation frequency of the Wave and Hopf modes (b), the intrinsic wavenumber of the Turing and Wave modes (c) on P_v. Other parameters are $D_u = 1.7$, $D_v = 12.1$, $D_w = 160$, $a = 1.15$, $b = 4.05$, $c = d = 1.5$, $\tau = 0.1$, $P_u = P_w = 0$.

The effect of the feedback intensity P_w on the intensities of the three modes is similar with that of P_u as shown in Fig. 5(a). The intensities of the Hopf and Wave modes decrease rapidly with P_w. This is because the new variable w represents an unreactive form of u. For Wave mode, the oscillation frequency and the intrinsic wavenumber increase with P_w (solid lines in Figs. 5(b) and 5(c)). For Hopf mode, the oscillation frequency increases with P_w (dash–dotted line in Fig. 5(b)). The control of the feedback intensity P_w on the oscillation frequency and the intrinsic wavenumber is opposite to that of P_u and P_v. So, by applying appropriate feedback intensities P_u, P_v, and P_w, one can control the intensities of the three modes (therefore the competition among them), the os-

cillation frequency and the intrinsic wavenumber of patterns, and obtain desirable spatiotemporal patterns.

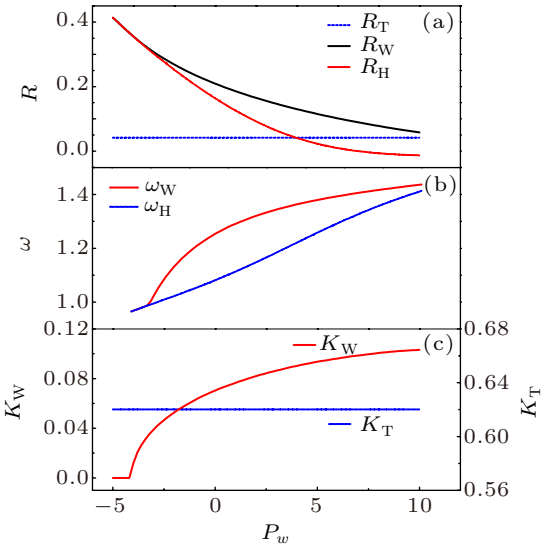


Fig. 5. (color online) Dependence of the intensities of the Turing, Hopf, and Wave modes (a), the oscillation frequency of the Hopf and Wave modes (b), the intrinsic wavenumber of the Turing and Wave modes (c) on P_w. Other parameters are $D_u = 1.7$, $D_v = 12.1$, $D_w = 160$, $a = 1.15$, $b = 4.05$, $c = d = 1.5$, $\tau = 0.1$, $P_u = P_v = 0$.

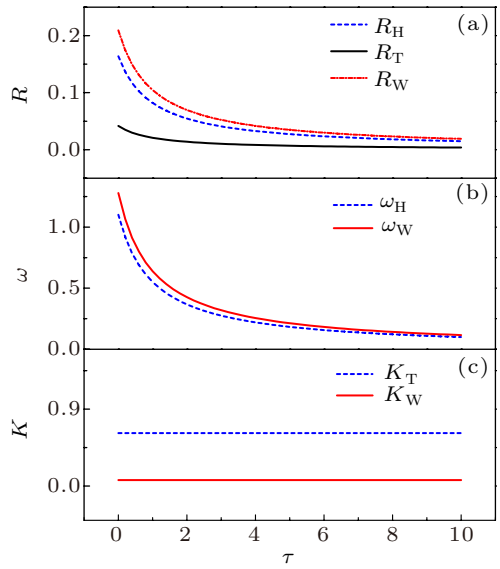


Fig. 6. (color online) Dependence of the intensities of the Turing, Hopf, and Wave modes (a), the oscillation frequency of the Hopf and Wave modes (b), the intrinsic wavenumber of the Turing and Wave modes (c) on τ. Other parameters are $D_u = 1.7$, $D_v = 12.1$, $D_w = 160$, $a = 1.15$, $b = 4.05$, $c = d = 1.5$, $P_u = P_v = P_w = 1.0$.

We also analyze the effect of delayed time τ on the three modes with fixed parameters $P_u = P_v = P_w = 1.0$. The competition among the three modes cannot be controlled by only changing the delayed time as shown in Fig. 6(a). However the oscillation frequency of the Hopf and Wave modes could change with the delayed time as shown by Fig. 6(b). In addition, the delayed time has no effect on the intrinsic wavenumber of the Turing and Wave modes as shown by Fig. 6(c). This is because that when the three feedback intensities are equal, $P_u = P_v = P_w = P$, we can define a new time scale $T = t/(1+\tau P)$, thus equation (11) can be rewritten as $\partial_T \Psi = Q + D\nabla^2 \Psi$. The time-delayed feedback is equivalent to rescaling the time scale of the system. Therefore, time-delayed feedback with identical intensities changes only the oscillatory frequencies of the Hopf and Wave modes, and it does not vary the intrinsic wavenumber of the Turing and Wave modes.

3. 2D numerical simulation

In order to verify the analytical results, we carry out two-dimensional (2D) numerical simulation of the model with time-delayed feedback by using the ADI (alternating directional iterative) method. The parameters of the system are: $a = 1.15$, $b = 4.05$, $c = d = 1.5$, $D_u = 1.7$, $D_v = 12.1$, $D_w = 160.0$. The simulations are performed on a square grid of 200×200 space units. The space step is $\Delta x = \Delta y = 0.4$ space units and the time step is $\Delta t = 0.02$ time units. The boundary conditions are taken to be no-flux. The simulations are started with a small random initial perturbation around the homogeneous steady states.

Figure 7 shows the transitions of spatiotemporal patterns controlled by different feedback parameters. As mentioned above, we choose the parameters to locate at the domain VI in Fig. 1, where the three instabilities coexist. In the absence of time-delayed feedback, the coexistence of the three modes result in the formation of mixed-mode patterns, as indicate in Figs. 7(c), 7(f), and 7(k). It can be seen that the Turing spots occupy only part of the medium. There exist several "holes" which contain oscillatory modes due to the Hopf and Wave instabilities. Then we apply appropriate time-delayed feedback to these patterns in Figs. 7(c), 7(f), and 7(k), and study how to control the pattern transition by time-delayed feedback. Figures 7(a)–7(d) show the transition of the patterns with increasing P_u ($P_v = P_w = 0$). It can been seen that the Turing spots occupy gradually the whole area with increasing P_u (Fig. 7(d)). If we decrease P_u the oscillatory modes will grow up and the wave pattern will gradually swallow the stationary Turing spots (Fig. 7(b)). Applying negative feedback with enough intensity, the wave pattern will dominant the whole domain (Fig. 7(a)). The simulation results are in accord with the above analytical results in Fig. 3.

Figure 7(e)–7(h) shows the development of a pattern with increasing P_v ($P_u = P_w = 0$): pure Turing mode (steady hexagon pattern) (Fig. 7(e))–three modes coexistence (Figs. 7(f)–7(g))–oscillatory modes (Hopf and Wave modes) (Fig. 7(h)). With increasing P_v the oscillatory mode becomes strong and dominant over the domain. The simulation results verify that the effect of P_v on the competition among the three modes is opposite to that of P_u as shown in Fig. 4.

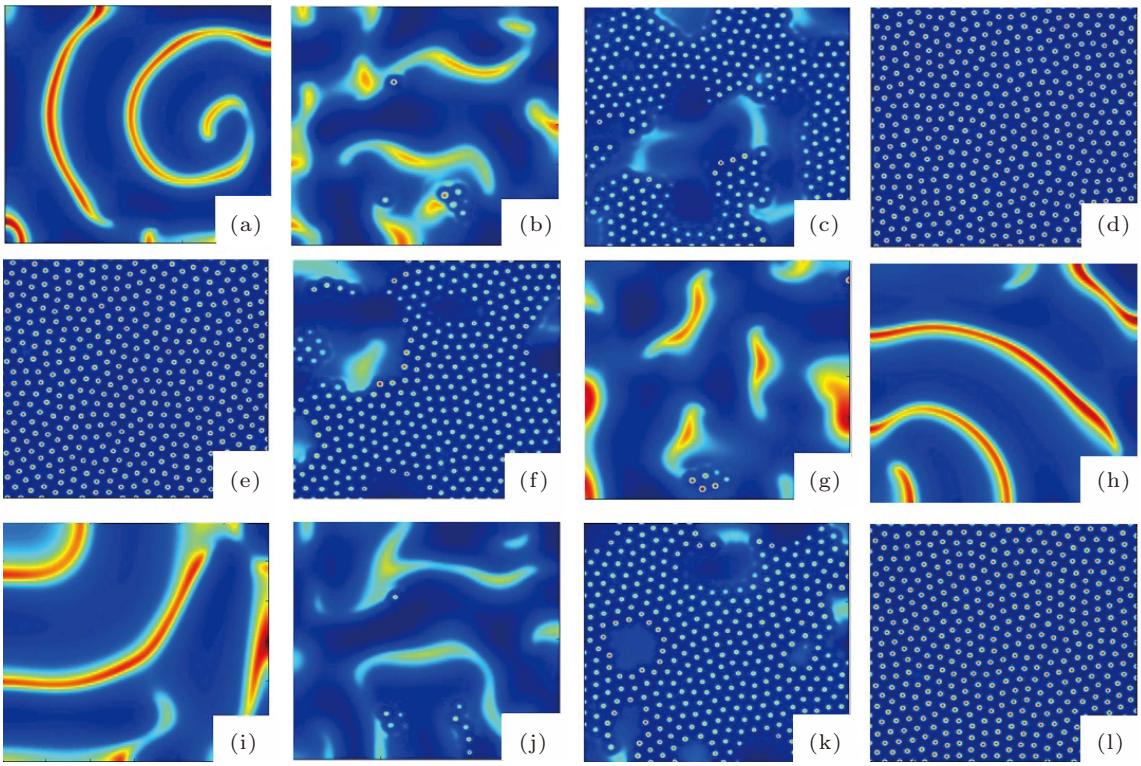


Fig. 7. (color online) Pattern transition at different feedback intensities. The feedback intensities P_u in panels (a)–(d) are -2.0, -0.6, 0.0, 1.0, respectively ($P_v = P_w = 0$); The feedback intensities P_v in panels (e)–(h) are -2.0, 0.0, 0.8, 1.6, respectively ($P_u = P_w = 0$); The feedback intensities P_w in panels (i)–(l) are -2.0, -0.6, 0.0, 1.0, respectively ($P_u = P_v = 0$). $\tau = 0.1$.

Figures 7(i)–7(l) show the evolvement of patterns from oscillatory modes to the stationary Turing mode with increasing P_w ($P_u = P_v = 0$). The simulation results reveal that the effect of P_w on controlling the pattern transition is equivalent to that of P_u. Both analyses and simulation results have shown that we can control the pattern formation by applying time-delayed feedback.

The analytical results shown in Figs. 1–6 shown above are obtained based on the linear stability analyses of Eq. (11) in which the delayed time τ should be a small value. For the case with large delayed time, these analyses are insufficient, and it could be further studied in terms of numerical simulations. Here, we find numerically that the dependence of the oscillation frequency and the intrinsic wavenumber of patterns on the feedback parameters is similar to that in the small delayed time case. So our results shown above are universal for any feedback parameters.

4. Conclusion

In this work we studied the control of pattern formation near codimension-three Turing–Hopf–Wave bifurcation by applying a strategy of time-delayed feedback in a three-variable Brusselator model. The time-delayed feedback is determined by the delayed time and feedback intensities. Based on the linear stability analysis, we find that the intensity, the oscillation frequency, and the intrinsic wavenumber of the three modes can be controlled by applying appropriate time-delayed feedback. Analytical results have shown that the oscillatory modes (Hopf and Wave modes) are enhanced with increasing P_v, however they are suppressed with increasing P_u and P_w. The oscillation frequencies of the Hopf and Wave modes and the intrinsic wavemunber of the Wave mode decrease with increasing P_u or P_v. However, they will increase with P_w. The role of P_v played on controlling the intensities of the three modes is opposite to that of P_u and P_w. The role of P_w played on controlling the oscillation frequencies and the intrinsic wavenumber is opposite to that of P_u and P_v. The characteristics of the Turing mode changes little by applying time-delayed feedback. By changing the delayed time τ with identical feedback intensities, the oscillation frequency of the Hopf and Wave modes can be controlled, however the competition among the three modes is unaffected. This is because applying identical intensities of feedback is equivalent to rescaling the time scale of the system. In summary, by applying appropriate feedback intensities and delayed time we can realize the control of the pattern formation near codimension-three Turing–Hopf–Wave bifurcations. Finally, we perform two-dimensional numerical simulation to confirm the analytical results.

The instability of the three-variable Brusselator model is determined by the parameters of the system, a, b, c, d, D_u, D_v, and D_w. In experiments, the spatial and temporal instabilities can be controlled by modulating these parameters. Our analytical results have shown that applying appropriate time-delayed feedback can also realize the control of the spatial and temporal instabilities. It illustrates that we can control the pat-

tern formation by applying time-delayed feedback rather than changing the parameters of the system. This becomes very useful in some experiments, in which the variation ranges of the parameters of the system are very limited. For example, the observed spatiotemporal patterns in the gas discharge system are obtained by changing mainly the parameter of the applied voltage. However, due to the limitation of the light-sensitive electrodes to high voltage, the applied voltage should be very low.[27,28] In order to obtain more patterns and extend the present study of pattern formation, one can use the strategy of time-delayed feedback to the gas discharge system even with the same light-sensitive electrodes, and just introducing a feedback loop composed of projector and computer.

References

[1] Cross M C and Hohenberg P C 1993 *Rev. Mod. Phys.* **65** 851
[2] Ouyang Q 2010 *Introduction of Nonlinear Science and Pattern Dynamics* (Beijing: Peking University Press) p. 130 (in Chinese)
[3] Zhang X M, Fu M L, Xiao J H and Hu G 2006 *Phys. Rev. E* **74** 015202
[4] Yang L F, Dolnik M, Zhabotinsky A M and Epstein I R 2002 *J. Chem. Phys.* **117** 7259
[5] Boissonade J, Dulos E and Kepper P D 1995 *Chemical Wave and Patterns* (Dirdrecht: Kluwer Press) p. 221
[6] Dong L F, Fan W L, Wang S, Ji Y F, Liu Z W and Chen Q 2011 *Phys. Plasmas* **18** 033506
[7] He Y F, Ai B Q and Liu F C 2013 *Phys. Rev. E* **87** 052913
[8] Guo W Q, Qiao C, Zhang Z M, Ouyang Q and Wang H L 2010 *Phys. Rev. E* **81** 056214
[9] Naknaimueang S, Allen M A and Müller S C 2006 *Phys. Rev. E* **74** 066209
[10] Kheowan O U, Zykov V S and Müller S C 2002 *Phys. Chem. Chem. Phys.* **4** 1334
[11] Zhang H, Cao Z J, Wu N J, Ying H P and Hu G 2005 *Phys. Rev. Lett.* **94** 188301
[12] Mikhailov A S and Showalter K 2006 *Phys. Rep.* **425** 79
[13] Chen J X, Xu J R, Yuan X P and Ying H P 2009 *J. Phys. Chem. B* **113** 849
[14] Schneider F M, Schöll E and Dahlem M A 2009 *Chaos* **19** 015110
[15] Stanton L G and Golovin A A 2007 *Phys. Rev. E* **76** 036210
[16] Handel A and Grigoriev R O 2005 *Phys. Rev. E* **72** 066208
[17] Sen S, Ghosh P, Riaz S S and Ray D S 2009 *Phys. Rev. E* **80** 046212
[18] He Y F, Ai B Q and Hu B B 2010 *J. Chem. Phys.* **133** 114507
[19] Liu F C, Wang X F, Li X C and Dong L F 2007 *Chin. Phys.* **16** 2640
[20] Ma J, Ying H P and Li Y L 2007 *Chin. Phys.* **16** 955
[21] Hu H X, Li Q S and Li S 2007 *Chem. Phys. Lett.* **447** 364
[22] Li Q S and Hu H X 2007 *J. Chem. Phys.* **127** 154510
[23] Wang H J and Ren Z 2011 *Commun. Theor. Phys.* **56** 339
[24] He Y F, Liu F C, Fan W L and Dong L F 2012 *Chin. Phys. B* **21** 034701
[25] Ghosh P 2011 *Phys. Rev. E* **84** 016222
[26] Vanag V K and Epstein I R 2002 *J. Phys. Chem. A* **106** 11394
[27] Dong L F, Li B, Lu N, Li X C and Shen Z K 2012 *Phys. Plasmas* **19** 052304
[28] Gurevich E L, Liehr A W, Amiranashvili S and Purwins H G 2004 *Phys. Rev. E* **69** 036211